NCAPD2 augments the tumorigenesis and progression of human liver cancer via the PI3K-Akt-mTOR signaling pathway

JIANG-XUE GU[1*], KE HUANG[1*], WEI-LIN ZHAO[1*], XIAO-MING ZHENG[2], YU-QIN WU[2], SHI-RONG YAN[3,4], YU-GANG HUANG[1] and PEI HU[1,5]

[1]Department of Laboratory Medicine and Department of Pathology, Taihe Hospital, Hubei University of Medicine, Shiyan, Hubei 442000, P.R. China; [2]Central Operating Room, Taihe Hospital, Hubei University of Medicine, Shiyan, Hubei 442000, P.R. China; [3]Hubei Key Laboratory of Embryonic Stem Cell Research, Hubei University of Medicine, Shiyan, Hubei 442000, P.R. China; [4]Hubei Key Laboratory of Wudang Local Chinese Medicine Research, School of Pharmaceutical Sciences, Hubei University of Medicine, Shiyan, Hubei 442000, P.R. China; [5]Institute of Biomedical Research, Hubei Clinical Research Center for Precise Diagnosis and Treatment of Hepatocellular Carcinoma, Taihe Hospital, Hubei University of Medicine, Shiyan, Hubei 442000, P.R. China

Received February 8, 2024; Accepted July 2, 2024

DOI: 10.3892/ijmm.2024.5408

Abstract. Non-SMC condensin I complex subunit D2 (*NCAPD2*) is a newly identified oncogene; however, the specific biological function and molecular mechanism of *NCAPD2* in liver cancer progression remain unknown. In the present study, the aberrant expression of NCAPD2 in liver cancer was investigated using public tumor databases, including TNMplot, The Cancer Genome Atlas and the International Cancer Genome Consortium based on bioinformatics analyses, and it was validated using a clinical cohort. It was revealed that NCAPD2 was significantly upregulated in liver cancer tissues compared with in control liver tissues, and *NCAPD2* served as an independent prognostic factor and predicted poor prognosis in liver cancer. In addition, the expression of NCAPD2 was positively correlated with the percentage of $Ki67^+$ cells. Finally, single-cell sequencing data, gene-set enrichment analyses and *in vitro* investigations, including cell proliferation assay, Transwell assay, wound healing assay, cell cycle experiments, cell apoptosis assay and western blotting, were carried out in human liver cancer cell lines to assess the biological mechanisms of NCAPD2 in patients with liver cancer. The results revealed that the upregulation of NCAPD2 enhanced tumor cell proliferation, invasion and cell cycle progression at the G_2/M-phase transition, and inhibited apoptosis in liver cancer cells. Furthermore, NCAPD2 overexpression was closely associated with the phosphatidylinositol 3-kinase (PI3K)-Akt-mammalian target of rapamycin (mTOR)/c-Myc signaling pathway and epithelial-mesenchymal transition (EMT) progression in HepG2 and Huh7 cells. In addition, upregulated *NCAPD2* was shown to have adverse effects on overall survival and disease-specific survival in liver cancer. In conclusion, the overexpression of NCAPD2 was shown to lead to cell cycle progression at the G_2/M-phase transition, activation of the PI3K-Akt-mTOR/c-Myc signaling pathway and EMT progression in human liver cancer cells.

Correspondence to: Professor Pei Hu or Professor Yu-Gang Huang, Department of Laboratory Medicine and Department of Pathology, Taihe Hospital, Hubei University of Medicine, 32 Renmin South Road, Shiyan, Hubei 442000, P.R. China
E-mail: hp2022jy@163.com.
E-mail: huangyg2018@outlook.com

*Contributed equally

Key words: non-SMC condensin I complex subunit D2, liver cancer, phosphatidylinositol 3-kinase-Akt-mammalian target of rapamycin, c-Myc, epithelial-mesenchymal transition, tumor survival and progression

Introduction

As liver cancer is the most prevalent primary liver neoplasm and the fourth leading cause of malignancy-associated death, it is considered one of the most aggressive tumors with notable morbidity and mortality rates, presenting a serious healthcare concern worldwide (1,2). The World Health Organization predicts that the worldwide incidence rate of liver cancer is increasing and may reach an annual incidence of ~1 million new cases in the next decade (3-5). Liver cancer is characterized by substantial molecular heterogeneity and a poor prognosis (6,7). Hence, the identification of reliable biomarkers to predict early or accurate prognosis, as well as the development of new molecular targeted therapeutic strategies for liver cancer is important.

Non-SMC condensin I complex subunit D2 (*NCAPD2*) is situated on chromosome 12p13.31 and is mainly expressed in the cytoplasm (8). It has been shown to mediate the recruitment and localization of mitosis-associated proteins on chromosomes, which mainly participate in chromosomal condensation and segregation during the process of the cell cycle, thus affecting cell mitosis (9,10). *NCAPD2* is a newly discovered, tumor-associated gene; however, studies on *NCAPD2* are limited. It has

been shown that *NCAPD2* expression is abnormally high and exerts an important role in numerous malignancies, such as colorectal cancer (11) and breast cancer (12), particularly triple-negative breast cancer (TNBC) (13). Furthermore, it has been revealed that *NCAPD2* is an independent prognostic indicator in liver cancer and is associated with positive clinical outcomes, mainly based on the results of bioinformatics analysis (14). However, the expression pattern, exact biological roles and molecular mechanisms of *NCAPD2* in liver cancer remain unknown.

In the current study, *NCAPD2* expression was investigated using public tumor databases, including The Cancer Genome Atlas (TCGA), TNMplot and the International Cancer Genome Consortium (ICGC). In addition, NCAPD2 expression was detected in clinical tissues and its functions were assessed using *in vitro* experiments. The results of the present study may provide increased knowledge on liver cancer and delineate the biological function of NCAPD2 in the progression of this type of cancer, which may be useful for identifying novel prognostic targets or developing anticancer therapeutic strategies for patients with liver cancer.

Materials and methods

NCAPD2 expression in liver cancer using public tumor databases. Three publicly available tumor databases, including TNMplot (differential gene expression analysis in tumor, healthy control and metastatic tissues, https://tnmplot.com/), TCGA (https://portal.gdc.cancer.gov/) and ICGC (https://dcc.icgc.org/), were used for the investigation of *NCAPD2* expression in liver cancer. From the TNMplot database (15), which uses gene chip or RNA-sequencing (RNA-seq) data to display the analysis of specific genes in selected tissue types, data from 379 paracancerous liver tissues and 806 primary liver cancer tissues were collected. TCGA-Genotype-Tissue Expression Project database was used to identify 50 paracancerous liver tissues and 374 liver cancer tissues. The ICGC database was used to identify 202 paracancerous liver tissues and 240 liver cancer tissues. The Human Protein Atlas (HPA, https://www.proteinatlas.org/) is a public database that was used to obtain proteome expression information of genes from 44 paracancerous control tissues and 18 tumor tissues. The HPA was used to investigate NCAPD2 protein expression in patients with liver cancer.

Clinical specimens. Clinical specimens were fixed in 10% neutral formalin at room temperature for 12-24 h and embedded in paraffin. A total of 33 formalin-fixed paraffin-embedded (FFPE) specimens, including 20 liver cancer and 13 paired adjacent non-cancerous liver samples, were collected for validation from the Department of Pathology, Taihe Hospital (Shiyan, China) between July and October 2023. The inclusion criteria of the clinical specimens were: i) Confirmation of liver cancer diagnosis by senior pathologists using tumor tissues from patients that did not undergo preoperative radiotherapy or chemotherapy; and ii) patients were free of other diseases, or their medical history revealed no other diseases apart from liver cancer.

Immunohistochemistry (IHC) and reverse transcription-quantitative PCR (RT-qPCR) assay. IHC detection of all FFPE slides was conducted using EliVision methods according to the manufacturers' instructions. Specifically, all 3-μm FFPE sections were dewaxed with xylene and rehydrated with graded ethanol. After antigen repair with EDTA (pH 9.0) in a pressure cooker for 4 min, endogenous peroxidase activity was blocked with 3% hydrogen peroxide in methanol for 10 min at room temperature. The slides were then incubated with primary antibodies (Table SI) at 37˚C for 1 h, were washed three times with PBS (3 min/wash), and were incubated with horseradish peroxidase (HRP)-labeled secondary antibody (cat. no. KIT-9923; Fuzhou Maixin Biotechnology Development Co., Ltd.) at 37˚C for 0.5 h. The nuclei were stained with hematoxylin for 30 sec and the sections were washed with water for bluing after 0.5% HCI-ethanol differentiation for 3 sec. Finally, chromogen detection was performed using DAB Plus Kit (cat. no. DAB-2032; Fuzhou Maixin Biotechnology Development Co., Ltd.) at room temperature for 10 min.

All IHC staining results were scanned and scored by at least two experienced pathologists. IHC staining of $NCPAD2^+$ cells was detected using light microscopy (magnification, x200 or x100) and these cells were graded based on quantity and intensity scores. Specifically, the quantity scoring criteria were: 0, absent; 1, ≤10%; 2, 11-50%; 3, 51-75%; 4, >75% and the intensity scoring criteria were: 0, no staining; 1, light yellow; 2, brownish yellow; 3, dark brown. The quantity and intensity scores were multiplied to yield an overall score ranging between 0 and 12. The percentage of $Ki67^+$ cells was calculated as the percentage of $Ki67^+$ cells to all cells in the field of view at low magnification (x200).

Additionally, total RNA was extracted from FFPE slides using the RNeasy FFPE kit (Qiagen GmbH) and total RNA was then used to synthesize first-strand cDNA using the First Strand cDNA Synthesis kit (Vazyme Biotech Co., Ltd.); these steps were performed according to the manufacturers' protocols. qPCR was carried out in an ABI Prism 7000 analyzer (Applied Biosystems; Thermo Fisher Scientific, Inc.) using Green Mix SYBR (Vazyme Biotech Co., Ltd.) and specific primers (Table SII) to determine mRNA expression. The thermocycling conditions were as follows: initial denaturation at 120 sec for 95˚C, followed by 40 cycles at 95˚C for 15 sec, 58˚C for 15 sec and 72˚C for 30 sec. GAPDH was used as an endogenous control. All experiments were performed in triplicate. The relative mRNA expression levels in liver cancer samples were determined using the $2^{-\Delta\Delta Cq}$ method (16). The primers were obtained from Sangon Biotech Co., Ltd.

Association analysis of NCAPD2 and clinicopathological signatures in liver cancer. The association between *NCAPD2* expression and the clinicopathological parameters of patients with liver cancer was assessed using TCGA-liver cancer data. All patients with liver cancer were divided into two subgroups based on median cut-off values; the high *NCAPD2* expression (n=187) and the low *NCAPD2* expression (n=187) groups. The distribution of *NCAPD2* expression in liver cancer in terms of age, pathological TNM (pTNM) stage, histological grades and survival status was plotted in an Sankey diagram. RNA-sequencing expression profiles and corresponding clinical information for liver cancer were downloaded from TCGA dataset. The package 'ggalluvial' of R software (version 4.2.1) was used to build Sankey diagram (17). Subsequently, the

prognostic analysis of *NCAPD2* expression in liver cancer was analyzed including overall survival (OS) or disease-specific survival (DSS) data from TCGA or the ICGC datasets based on Kaplan-Meier and log-rank test. Furthermore, univariate Cox (uni-cox) and multivariate Cox (multi-cox) regression analyses were applied to investigate the relationship between *NCAPD2* expression and other clinicopathological signatures in TCGA-liver cancer data.

Immune infiltration and gene-set enrichment analysis (GSEA). Estimation of STromal and Immune cells in MAlignant Tumor tissues using Expression data (ESTIMATE) assesses mesenchymal and immune cells in malignant tumors using gene expression data. The algorithm scores specific sets of genes by GSEA to obtain the stromal and the immune scores of the tumor sample, and these two scores are added together to obtain the ESTIMATE score, which can be used to estimate tumor purity. With the ESTIMATE algorithm, stromal and immune scores can be obtained for every sample, and then the tumor samples can be classified into high- and low-expression subgroups based on these scores, facilitating subsequent bioinformatics analysis and research. Specifically, immune infiltration analyses of the ESTIMATE algorithm, including stromal and immune scores, and the ESTIMATE score were conducted via the 'estimate' (version 1.0.13) package (18) in R (version 4.2.1) software (https://www.r-project.org/). Furthermore, the evaluation of immune cell abundance was derived from the GSEA algorithm provided in the R package 'GSVA' (version 1.46.0) (19). For GSEA, the R package GSVA (20,21) was used to investigate the underlying molecular mechanisms of *NCAPD2* in TCGA-liver cancer data. Spearman's correlation coefficient was used to denote the correlation between genes and pathway scores. Thresholds were set at Spearman's correlation coefficient, r_s>0.5. P<0.05 was considered to indicate a statistically significant difference.

Single-cell sequencing analysis. Integrated iMMune profiling of large adaptive CANcer patient cohorts (IMMUcan), an online service platform established by a team of researchers from the Institute of Research Saint-Louis (Paris, France), collects single-cell sequencing data of >56 cancer types worldwide, and aims to create and integrate the clinical, cellular and molecular profile of different tumor types and the tumor immune microenvironment (22). The IMMUcan database provides detailed clinical annotations that link cell types and gene expression patterns to specific clinical patterns. It also provides extensive functionality for analyzing multiple datasets. The single-cell RNA-seq datasets GSE140228 (23) and GSE112271 (24) from the Gene Expression Omnibus dataset (https://www.ncbi.nlm.nih.gov/geo/; Table SIII) were used to characterize *NCAPD2* expression in different cell clusters from liver cancer.

Construction of NCAPD2 interference and overexpression systems. NCAPD2 expression was assessed in the liver cancer cell lines Huh7 (cat. no. CL-0120; Procell Life Science & Technology Co. Ltd.), MHCC-97H (cat. no. TCH-C258; HyCyte), HepG2 (cat. no. CL-0103; Procell Life Science & Technology Co. Ltd.) and LM3 (cat. no. TCH-C456; HyCyte). All cell lines used in the current study were authenticated using short tandem repeat profiling. *In vitro* assays involving HepG2 cells with small interfering RNA (siRNA)-induced NCAPD2 knockdown using si-NCAPD2, or Huh7 cells with pcDNA-NCAPD2 plasmid-induced NCAPD2 overexpression were performed to discover the molecular mechanisms of NCAPD2 in liver cancer.

Cell culture. The liver cancer cell lines HepG2, Huh7, MHCC-97H and LM3 were cultured in basic DMEM (cat. no. C11995500BT; Gibco; Thermo Fisher Scientific, Inc.) supplemented with 10% fetal bovine serum (Gibco; Thermo Fisher Scientific, Inc.) at 37˚C and 5% CO_2. The culture medium was replaced every 2-3 days until cell density reached >90% for passaging, and cells in the logarithmic growth phase were used for RT-qPCR and subsequent experiments.

Cell transfection. When cell density reached ~70%, 50 nmol plasmids or 50 nmol siRNAs were transfected into liver cancer cells using Lipofectamine® 3000 (Invitrogen; Thermo Fisher Scientific, Inc.) according to the manufacturer's instructions. Huh7 cells were transfected with the NCAPD2 overexpression plasmid pcDNA3.1-NCAPD2 (Zhuhai DL Biotech Co., Ltd.), and pcDNA3.1 was used as a control. HepG2 cells were transfected with si-NCAPD2 (Guangzhou Ribobio Co., Ltd.; Table SII), and si-negative control (NC) was used as a control. All cell line experiments were performed at 37˚C. The culture medium was refreshed 6 h after transfection, and most other experiments (RT-qPCR, cell proliferation, flow cytometry, cell invasion, cell migration experiments, etc.) were carried out 24 h post-transfection, with the exception of western blotting, which was carried out 48 h post-transfection. The experiments were performed in triplicate.

RT-qPCR. Total RNA was extracted from cell lines using TRIzol® reagent (Invitrogen; Thermo Fisher Scientific, Inc.), according to the manufacturer's instructions. Total RNA was used to synthesize first-strand cDNA using the First Strand cDNA Synthesis kit and qPCR was carried out as aforementioned.

Cell proliferation. A total of 5,000 cells/well were cultured in 96-well plates, and MTT reagent (20 μl/well; Sigma-Aldrich; Merck KGaA) was added at 24, 48 and 72 h in the dark. The supernatant was removed after 4 h of incubation and DMSO (150 μl/well; Sigma-Aldrich; Merck KGaA) was added. Optical density was measured at 495 nm.

Transwell assay. Cells were cultured in 12-well plates for 24 h, and were then digested with trypsin and counted. Cell suspensions were prepared using serum-free medium to ensure cell density was $5x10^4$ cells/well and were seeded into Transwell cell culture chambers (24-well; pore size, 8 μm; cat. no. 3422; Corning, Inc.). For the cell invasion experiments, Matrigel (cat. no. 356234; Corning, Inc.) was diluted and spread evenly in the upper chamber, and was incubated at 37˚C overnight. Subsequently, 200 μl cell suspension was added to the upper chamber, 600 μl DMEM supplemented with 10% fetal bovine serum was added to the lower chamber, and the cells were incubated at 37˚C for 24 h, after which, images were captured. For the cell migration experiments, the same steps were performed as for the invasion assay; however, Matrigel-free chambers were used. Subsequently, the chambers were fixed with anhydrous methanol for 30 min, stained with 0.1% crystal violet for 20 min at room temperature and finally washed with double-distilled water three times. Images

were captured under a light microscope after the chambers were dried to observe cell migration and invasion.

Wound healing assay. Cells were cultured in 6-well plates for 24 h to achieve uniform coverage of the entire culture plate, and were then scratched vertically with a 200-μl pipette tip, washed three times with PBS and cultured in serum-free medium. Cell migration was observed at 0 and 48 h; images of the cells were captured under a light microscope and cell migration was analyzed using ImageJ (version 1.8.0; National Institutes of Health). Cell migration rate (%)=(0 h scratch area -48 h scratch area)/0 h scratch area x100.

Flow cytometry. For the cell cycle experiments, cells were digested with 0.25% trypsin-EDTA solution, centrifuged for 100 x g at room temperature for 5 min, and the cell precipitates were collected and washed twice with PBS. Subsequently, $1.0x10^4$ cells were fixed with 70% ethanol at 4˚C overnight, and were then incubated with 100 mg/l RNase A and 50 mg/l PI solution (Beyotime Institute of Biotechnology) at 37˚C for 30 min in the dark. Cell cycle progression was assessed using a flow cytometer (FACSCalibur; BD Biosciences), and the proportion of cells in each phase of the cell cycle was analyzed using FlowJo7.6 software (FlowJo LLC).

For the cell apoptosis assay, the same trypsin digestion was performed as for cell cycle experiments; subsequently, the precipitate was collected and $1.0x10^4$ cells were washed twice with PBS and resuspended in 100 μl PBS. Cells were then incubated with 8 μl FITC staining solution for 15 min at room temperature and 2 μl PI staining solution for 5 min at room temperature in the dark, according to the instructions of the Annexin V-FITC/PI Apoptosis Double Staining kit (cat. no. 556547; BD Biosciences). Finally, the apoptotic rate was analyzed by flow cytometry (FACSCalibur) using FlowJo7.6 software.

Western blotting. Cells were lysed using RIPA lysis buffer (Beyotime Institute of Biotechnology) and were placed on ice for 30 min before the cell lysates were centrifuged at 4˚C for 15 min. Protein concentration was determined using the BCA assay (Beyotime Institute of Biotechnology). Subsequently, proteins were incubated for 10 min in loading buffer, and 30 μg protein/lane was separated by SDS-PAGE on 10% gels and transferred to PVDF membranes (MilliporeSigma). The membranes were incubated with 5% skimmed milk powder at room temperature for 2 h, and TBS-1% Tween-20 (TBST; neoFroxx GmbH) was used to wash the membrane three times (10 min/wash). Finally, the membranes were incubated with diluted primary antibodies (Table SI) overnight at 4˚C, washed three times with TBST and then incubated with HRP-linked secondary antibodies (1:5,000; anti-rabbit/mouse IgG; cat. nos. 7074s and 7076s; Cell Signaling Technology, Inc.) for 2 h at room temperature. The blots were visualized on a gel imager (Bio-Rad Laboratories, Inc.) using an enhanced chemiluminescence substrate kit (cat. no. BL523B; Biosharp Life Sciences).

Statistical analysis. All statistical analyses were performed using GraphPad Prism (version 8.0; Dotmatics). Data are expressed as the mean ± SD and all *in vitro* experiments were performed in triplicate. Paired Student's t-test was used to determine the significance of differences between two paired groups. Unpaired Student's t-test was used to determine the significance of differences between two independent groups. To compare multiple groups, one-way ANOVA followed by Bonferroni test was used. In addition, the χ^2 test, Fisher's exact test and log-rank test were used, and non-parametric data were analyzed using Mann-Whitney U test and Spearman's correlation coefficient. $P<0.05$ was considered to indicate a statistically significant difference.

Results

NCAPD2 is upregulated in liver cancer compared with in control liver tissues. Based on the TNMplot, TCGA and ICGC databases, bioinformatics analyses revealed that the mRNA expression levels of *NCAPD2* were upregulated in liver cancer tissues compared with those in healthy control liver tissues (Fig. 1A-D). Furthermore, *NCAPD2* mRNA expression was upregulated in liver cancer tissues compared with in paired healthy control tissues (Fig. 1C). In terms of NCAPD2 protein expression, the HPA dataset indicated that NCAPD2 was markedly upregulated in liver cancer tissues compared with in healthy control tissues (Fig. 1E).

Clinical validation of NCAPD2 expression in patients with liver cancer. For the validation of NCAPD2 expression in patients with liver cancer, 20 liver cancer tissues and 13 adjacent non-cancerous samples were collected for IHC. The results suggested that NCAPD2 was significantly higher in liver cancer tissues than in adjacent non-cancerous tissues in terms of protein (Fig. 2A and B) and mRNA expression levels (Fig. 2C).

NCAPD2 expression is positively correlated with Ki67$^+$ cells in liver cancer. As a cell proliferation index, Ki67 was used to investigate the relationship between *NCAPD2* expression and Ki67$^+$ cells in liver cancer. It was suggested that NCAPD2 expression, namely NCAPD2 IHC score, was positively correlated with the proportion of Ki67$^+$ cells (Fig. 3A and B). In addition, based on TCGA-liver cancer data, *NCAPD2* expression was positively correlated with the expression of *MKI67*, the gene symbol of Ki67 (Fig. 3C).

Analysis of the association between NCAPD2 expression and clinicopathological characteristics in liver cancer. The association of *NCAPD2* and clinicopathological parameters in liver cancer revealed that *NCAPD2* expression was significantly associated with age, pTNM stage (especially T stage), histological grade and α-fetoprotein (AFP; $P<0.001$), but not with sex, BMI, residual tumor and Ishak fibrosis score (25) (Table SIV). In addition, an alluvial diagram showed the distribution of *NCAPD2* expression in terms of age, pTNM stage, histological grade and survival status (Fig. 4A). It suggested that *NCAPD2* expression was related to age, pTNM stage, histological grade and survival status in liver cancer. Furthermore, *NCAPD2* expression was upregulated in patients with advanced pTNM stage or advanced histological grade liver cancer, or in those with higher AFP levels (>400 ng/ml) compared with in the control subgroups (Fig. 4B-D). Subsequently, the prognostic analysis revealed that upregulation of *NCAPD2* was associated with poor OS and DSS based on TCGA data (Fig. 4E and F) or ICGC data (Fig. 4G). The uni-cox and multi-cox

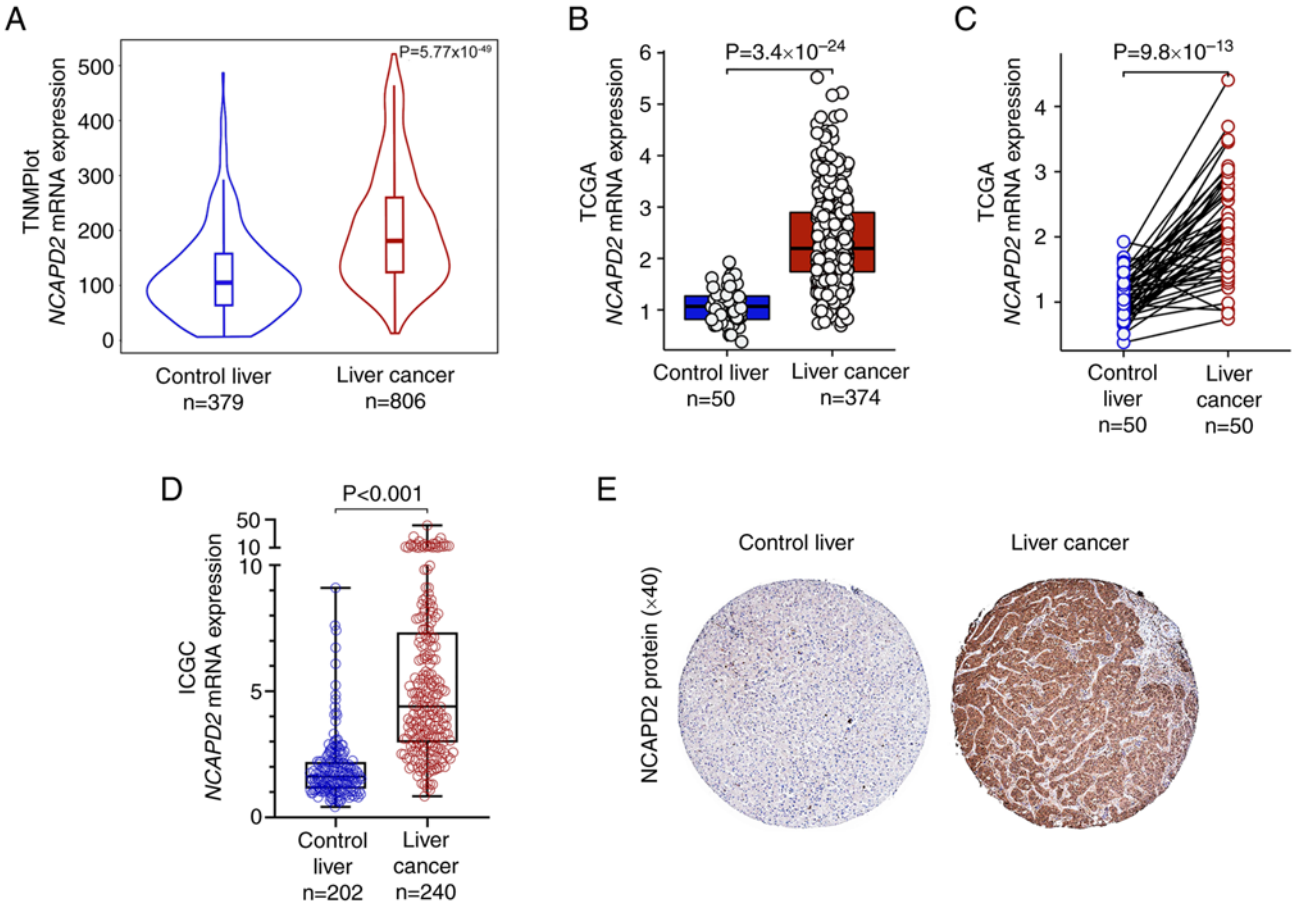

Figure 1. Aberrant expression of NCAPD2 in liver cancer. NCAPD2 expression in liver cancer compared with control liver tissues based on the (A) TNMplot, (B) unpaired TCGA (C) paired TCGA and (D) ICGC datasets, and (E) HPA platform; x40 magnification. HPA, Human Protein Atlas; ICGC, International Cancer Genome Consortium; NCAPD2, non-SMC condensin I complex subunit D2; TCGA, The Cancer Genome Atlas.

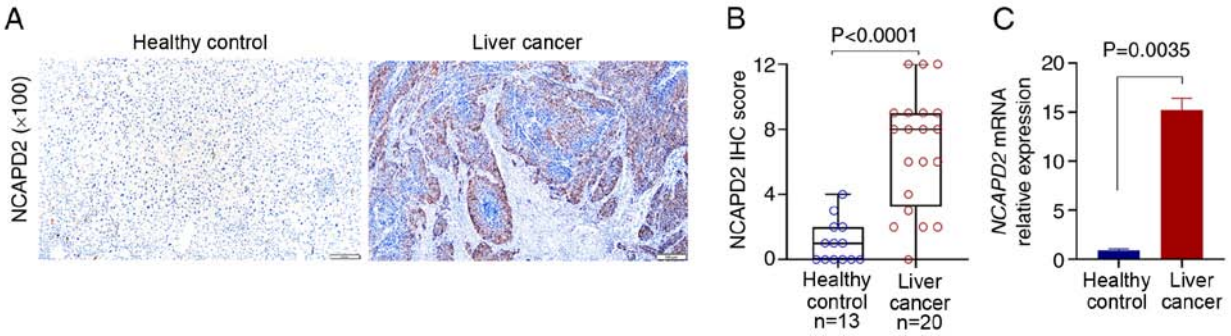

Figure 2. Expression of NCAPD2 in clinical liver cancer samples. (A) IHC image of NCAPD2 in liver cancer and healthy control tissues; x100 magnification. (B) IHC score of NCAPD2 in liver cancer and healthy control tissues. (C) Relative mRNA expression levels of *NCAPD2* in liver cancer and healthy control tissues. IHC, immunohistochemistry; NCAPD2, non-SMC condensin I complex subunit D2.

regression analyses indicated that *NCAPD2* expression was strongly associated with prognosis, and may serve as an independent prognostic marker of OS in patients with liver cancer (Table SV). Furthermore, among the common types of gene mutations in liver cancer based on TCGA dataset, including *TP53* and *CTNNB1* mutations, the analysis showed that *NCAPD2* expression was increased in *TP53* mutant (mut) compared with in *TP53* wild-type (wt) liver cancer (Fig. 4H). The expression of *NCAPD2* was not associated with *CTNNB1* mutation (Fig. 4I).

Immune infiltration analysis and gene-enriched pathways of NCAPD2 in liver cancer. Immune infiltration assays suggested that the stromal score was significantly lower in the high *NCAPD2* expression group compared with that in the low *NCAPD2* expression group, but no difference was observed for the immune score or ESTIMATE score (Fig. 5A). Subsequently, the GSEA algorithm revealed that the abundance of most immune cells was not related to differences in the expression of *NCAPD2*, with the exception of dendritic cells and T helper (Th) cells (especially Th2 and Th17 cells) (Fig. 5B). Moreover,

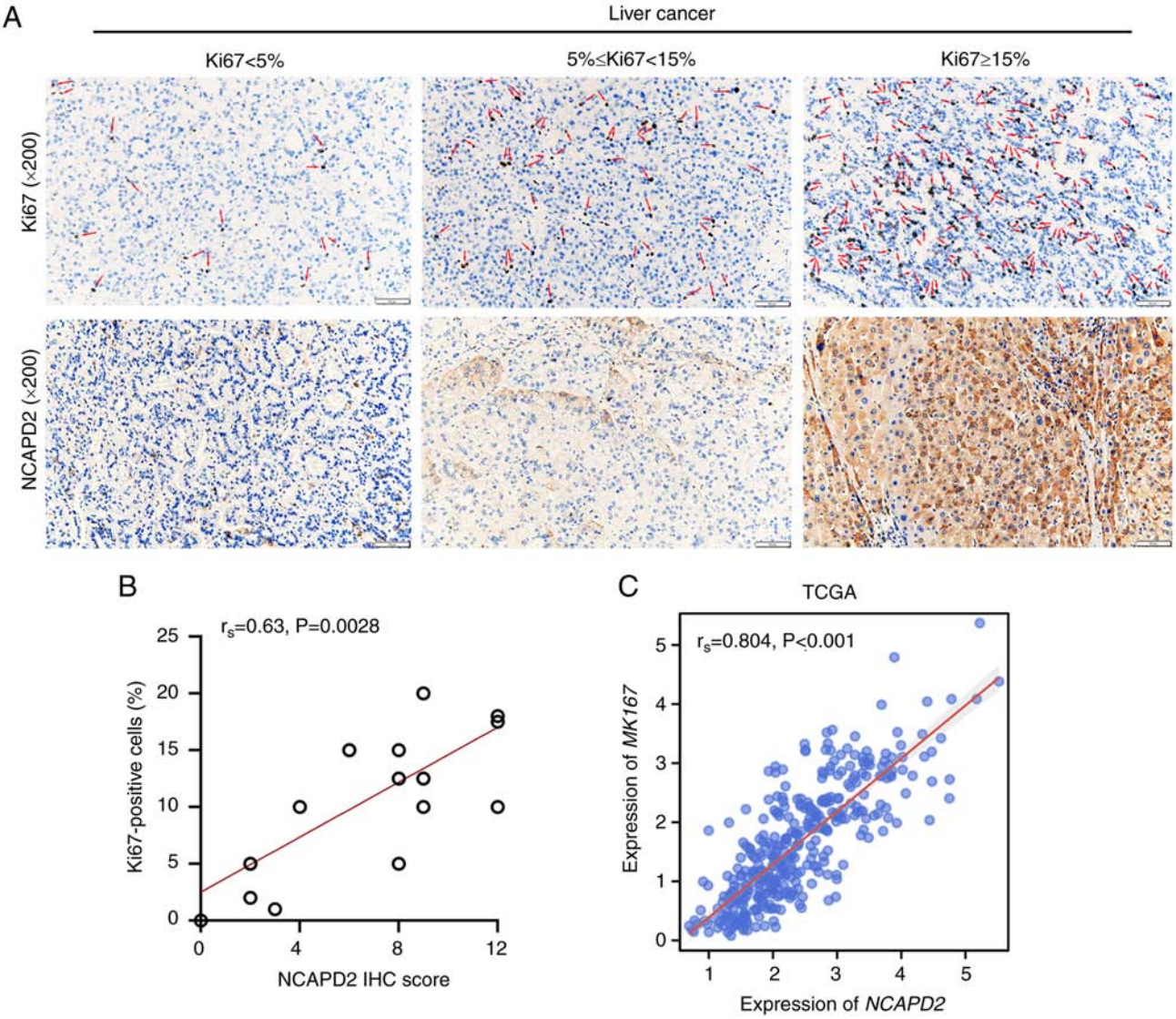

Figure 3. NCAPD2 expression is positively correlated with the cell proliferation index, Ki67. (A) IHC images of NCAPD2 and Ki67 expression in liver cancer; x200 magnification. (B) NCAPD2 IHC score was positively correlated with the proportion of Ki67$^+$ cells in terms of protein expression. Red arrows indicate Ki67$^+$ cells. (C) Based on TCGA-liver cancer data, *NCAPD2* expression was positively correlated with that of *MKI67* in terms of mRNA expression. IHC, immunohistochemistry; NCAPD2, non-SMC condensin I complex subunit D2; TCGA, The Cancer Genome Atlas.

the GSEA asserted that liver cancer with high *NCAPD2* expression was mostly enriched in the phosphatidylinositol 3-kinase (PI3K)-Akt-mammalian target of rapamycin (mTOR) signaling pathway, the tumor proliferation signature, the G_2/M checkpoint of the cell cycle and Myc signal targets (Fig. 5C). In the GSE140228 dataset, the high expression subgroup of *NCAPD2* was mainly enriched in the cell population in the cell cycling state (Fig. 5D); the GSE112271 dataset denoted that *NCAPD2* was mainly expressed in the malignant cell population (Fig. 5E).

Aberrant NCAPD2 expression alters cell proliferation, invasion, cell cycle progression and apoptosis in liver cancer cells. NCAPD2 expression was assessed in the liver cancer cell lines Huh7, MHCC-97H, HepG2 and LM3. Among these four liver cancer cell lines, the mRNA and protein expression levels of NCAPD2 were highest in HepG2 cells and lowest in Huh7 cells (Fig. 6A and B). Thus, HepG2 cells were selected for siRNA experiments and Huh7 cells were selected for overexpression experiments to further investigate the biological roles of NCAPD2 in liver cancer. Notably, the mRNA and protein expression levels of NCAPD2 were significantly inhibited in HepG2 cells transfected with si-NCAPD2 compared with those transfected with si-NC (Fig. 6C and D). By contrast, the mRNA and protein expression levels of NCAPD2 were significantly upregulated in Huh7 cells transfected with pcDNA-NCAPD2 compared with those transfected with pcDNA3.1. Specifically, NCAPD2 knockdown significantly inhibited the proliferation (Fig. 6E), invasion and migration (Fig. 6G and I) of HepG2 cells transfected with si-NCAPD2 compared with those transfected with si-NC. Flow cytometry showed that NCAPD2 knockdown significantly enhanced the apoptosis of HepG2 cells (8.88 vs. 11.1%; Fig. 6K). By contrast, overexpression of NCAPD2 increased the proliferation (Fig. 6F), invasion and migration (Fig. 6H and J) of Huh7 cells transfected with pcDNA-NCAPD2 compared

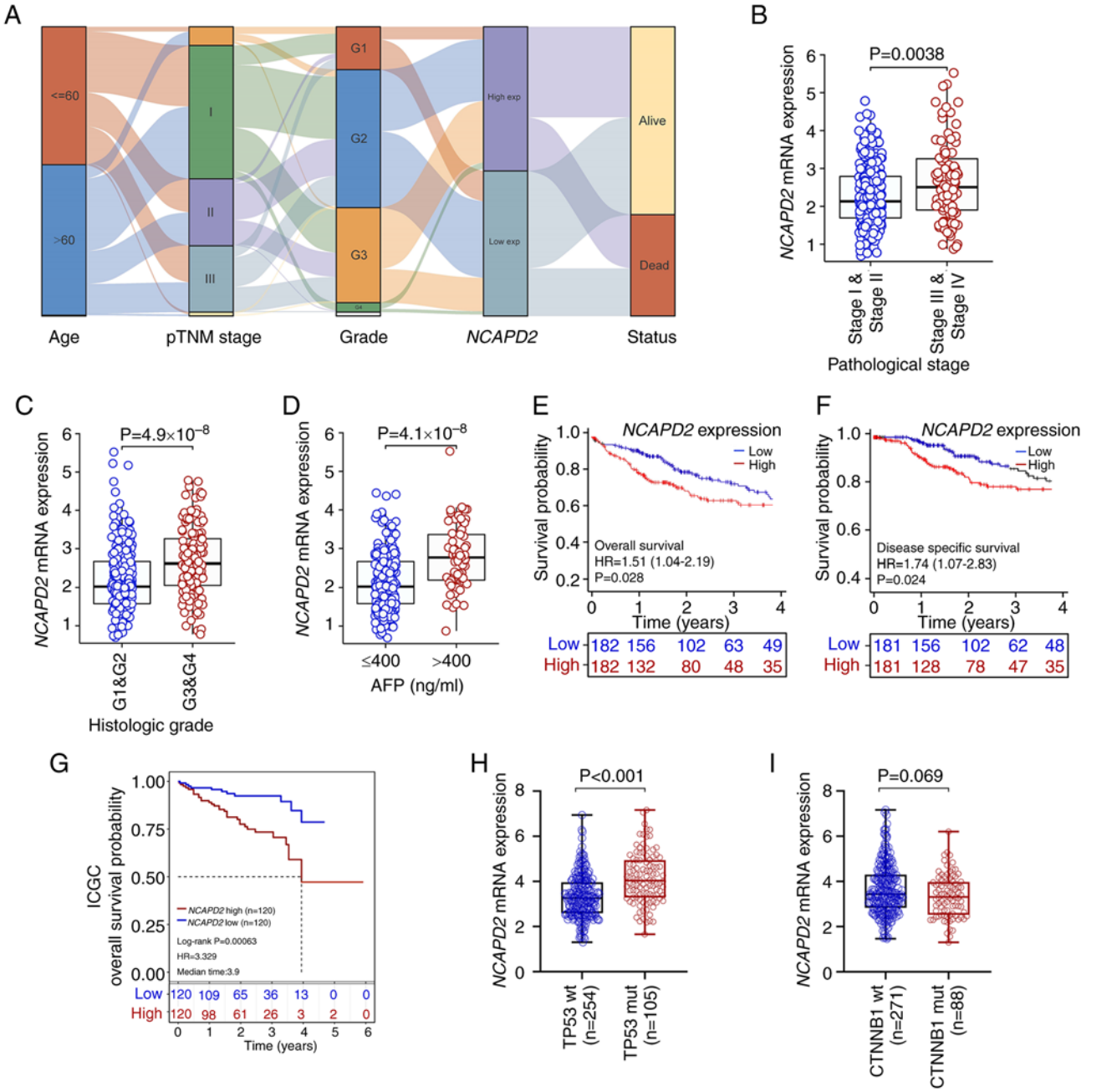

Figure 4. Association between *NCAPD2* expression and clinicopathological signatures in liver cancer. (A) Alluvial diagram was used to display the distribution of *NCAPD2* expression in liver cancer in terms of age, pTNM stage, histological grade and survival status. Differences in *NCAPD2* expression regarding clinicopathological parameters, including (B) pTNM stage, (C) histological grade and (D) AFP concentration. Prognostic analysis of *NCAPD2* expression in liver cancer, including (E) overall survival and (F) disease-specific survival, based on TCGA data. (G) Prognostic analysis of *NCAPD2* expression in liver cancer overall survival, based on the ICGC dataset. Differences in *NCAPD2* expression regarding different types of gene mutations in liver cancer, including (H) *TP53* and (I) *CTNNB1* mutations. AFP, α-fetoprotein; ICGC, International Cancer Genome Consortium; mut, mutant; *NCAPD2*, non-SMC condensin I complex subunit D2; pTNM, pathological TNM; TCGA, The Cancer Genome Atlas; wt, wild-type.

with those transfected with pcDNA3.1. Flow cytometry also showed that NCAPD2 overexpression impeded the apoptosis of Huh7 cells (10.95 vs. 6.76%; Fig. 6L).

NCAPD2 promotes cell cycle progression at the G_2/M-phase transition, activates the PI3K-Akt-mTOR signaling pathway and epithelial-mesenchymal transition (EMT) progression in liver cancer cells. Flow cytometry revealed that knockdown of NCAPD2 inhibited the cell cycle at the G_2/M-phase transition and enhanced G_0/G_1-phase transition in HepG2 cells (Fig. 7A), whereas overexpression of NCAPD2 boosted the cell cycle at the G_2/M-phase transition in Huh7 cells (Fig. 7B). Western blotting revealed that knockdown of NCAPD2 expression suppressed the expression levels of c-Myc; affected the expression levels of EMT-related proteins, including upregulation of E-cadherin, and downregulation of N-cadherin and vimentin; and reduced the phosphorylation of mTOR, PI3K and Akt in HepG2 cells. By contrast, NCAPD2 overexpression enhanced the expression levels of c-Myc; activated the EMT via altering the expression levels of the related proteins,

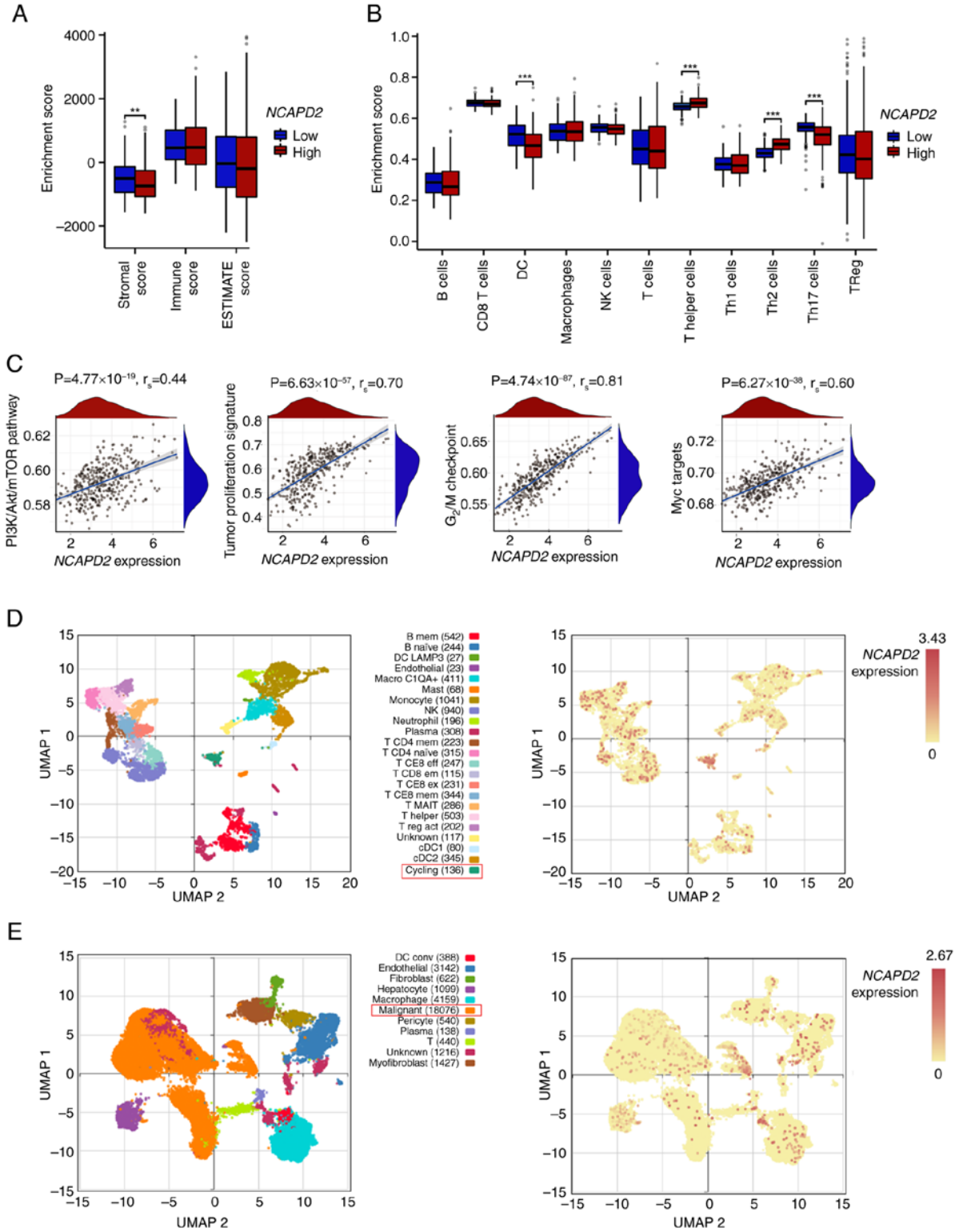

Figure 5. Immune infiltration and GSEA of *NCAPD2* in liver cancer. (A) Immune infiltration analyses of the ESTIMATE algorithm, including stromal score, immune score and ESTIMATE score in liver cancer with high and low *NCAPD2* expression. (B) Immune cell abundance of high or low *NCAPD2* expression groups in liver cancer. (C) GSEA for the *NCAPD2*-related signaling pathways in liver cancer. Single-cell sequencing analysis of *NCAPD2* expression in liver cancer derived from (D) GSE140228 and (E) GSE112271 datasets. **P<0.01, ***P<0.001. ESTIMATE, Estimation of STromal and Immune cells in MAlignant Tumor tissues using Expression data; GSEA, gene-set enrichment analysis; mTOR, mammalian target of rapamycin; *NCAPD2*, non-SMC condensin I complex subunit D2; PI3K, phosphatidylinositol 3-kinase.

including downregulation of E-cadherin, and upregulation N-cadherin and vimentin; and increased the expression levels of phosphorylated (p)-mTOR, p-PI3K and p-Akt in Huh7 cells (Fig. 7C).

Discussion

Condensin complexes exert an essential function in the process of chromosomal condensation in eukaryotic organisms,

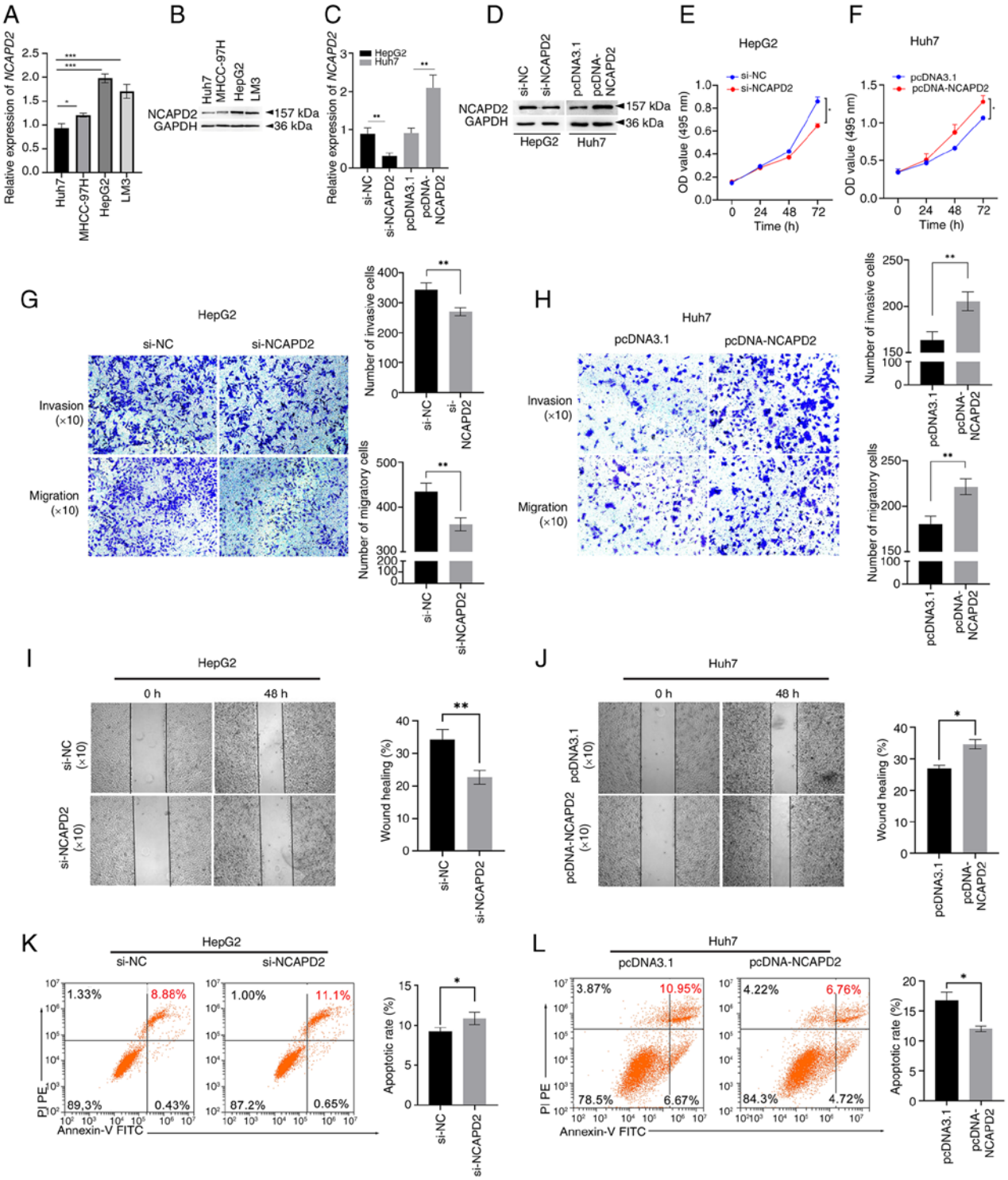

Figure 6. Aberrant NCAPD2 expression affects cell proliferation, invasion and apoptosis in liver cancer cell lines. (A) mRNA and (B) protein expression levels of NCAPD2 expression in the liver cancer cells Huh7, MHCC-97H, HepG2 and LM3. (C) mRNA and (D) protein expression levels of NCAPD2 in si-NCAPD2-transfected HepG2 cells and pcDNA-NCAPD2 overexpression plasmid-transfected Huh7 cells. MTT assay of transfected (E) HepG2 and (F) Huh7 cells. Cell invasion and migration assays of transfected (G) HepG2 and (H) Huh7 cells; x10 magnification. Wound healing assay of transfected (I) HepG2 and (J) Huh7 cells; x10 magnification. Apoptosis analysis of transfected (K) HepG2 and (L) Huh7 cells. All the experiments were performed in triplicate. *P<0.05, **P<0.01, ***P<0.001. NC, negative control; NCAPD2, non-SMC condensin I complex subunit D2; si, small interfering.

and two types of condensin complexes exist in vertebrates: Condensin complex I and II (13). *NCAPD2*, as a subunit of condensin complex I, not only exerts a vital function in chromatin condensation and segregation during cell proliferation, but is also involved in maintaining genome stability (10,26). As previously reported (12-14,27-31), *NCAPD2* is commonly expressed in healthy control tissues, such as lymph nodes, bone marrow and fat. Under pathological conditions, aberrant expression of *NCAPD2* is strongly associated with the incidence of cancer and non-tumorigenic diseases. In addition,

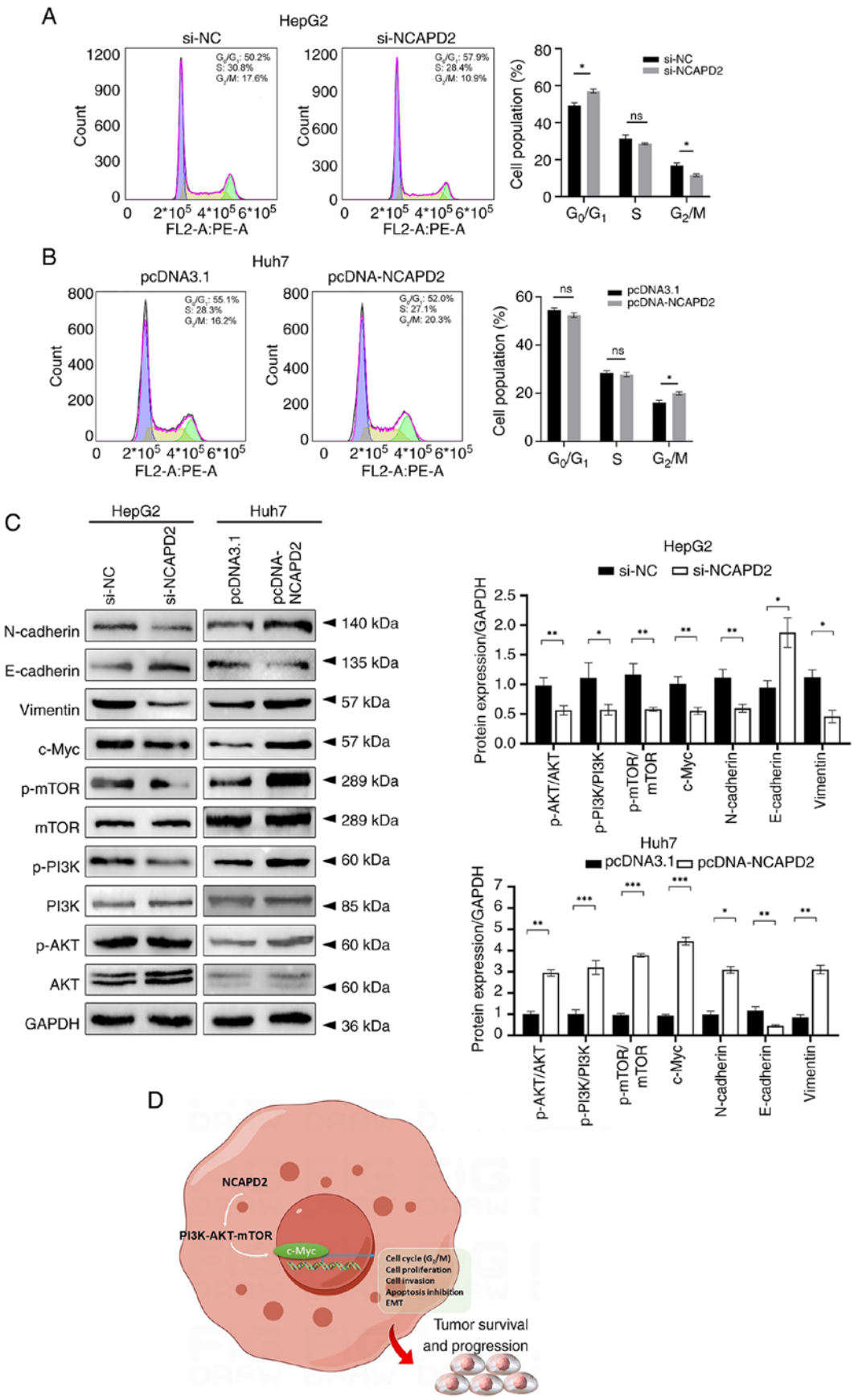

Figure 7. NCAPD2 promotes cell cycle progression at the G2/M-phase transition, activates the PI3K-Akt-mTOR and c-Myc signaling pathways, and induces EMT progression in liver cancer cell lines. Cell cycle assay of (A) si-NCAPD2-transfected HepG2 cells and (B) pcDNA-NCAPD2 overexpression plasmid-transfected Huh7 cells. (C) Western blotting of proteins related to the PI3K-Akt-mTOR/c-Myc signaling pathway and EMT progression after silencing of NCAPD2 in HepG2 cells or overexpression of NCAPD2 in Huh7 cells. All the experiments were performed in triplicate. (D) Diagram of the molecular mechanism. *P<0.05, **P<0.01, ***P<0.001. EMT, epithelial-mesenchymal transition; mTOR, mammalian target of rapamycin; NC, negative control; NCAPD2, non-SMC condensin I complex subunit D2; p-, phosphorylated; PI3K, phosphatidylinositol 3-kinase; si, small interfering.

NCAPD2 harbors a critical effect on central nervous system development. Zhang *et al* (27) demonstrated the association between *NCAPD2* polymorphisms and Parkinson's disease. Lin *et al* (28) found that a typical splice-site variant in the *NCAPD2* gene (c.3477+2T>C) may be associated with primary microcephaly. Upregulation of *NCAPD2* has also been shown to induce an inflammatory response through the IKK/NF-κB pathway in ulcerative colitis (29), and a recent study identified *NCAPD2* as a novel biomarker for the unfavorable prognosis of lung adenocarcinoma, related to immune infiltration and tumor mutational burden (30). He *et al* (12) revealed that *NCAPD2* may contribute to breast cancer cell progression via CDK1-related signaling. Zhang *et al* (13) showed that interference with *NCAPD2* expression may cause G_2/M arrest through the p53 signaling pathway, leading to cell proliferation inhibition, polyploidy and apoptosis, and reduced invasiveness of TNBC cells. In liver cancer, fewer studies have been performed related to *NCAPD2*. It has been suggested that *NCAPD2* is one of the hub genes that might serve vital roles in the progression of liver cancer through an integrated bioinformatics assay (31). Furthermore, Dong *et al* (14) performed a pan-cancer analysis and asserted that *NCAPD2* may act as a prognostic marker in various types of cancer, including liver cancer. These previous findings indicated that *NCAPD2* may be an independent factor that can predict poor survival in liver cancer, which is mainly involved in the G_2/M checkpoint and p53 signaling pathway.

Compared with the aforementioned studies, in the present study, liver cancer data from the public databases TNMplot, TCGA and ICGC were integrated, the expression and prognostic value of *NCAPD2* in patients with liver cancer was analyzed, and the results were validated in clinical samples. Additionally, immune infiltration assays and single-cell sequencing analysis showed that *NCAPD2* expression was not significantly associated with immune infiltration, but was associated with stromal score. In liver cancer, overexpression of *NCAPD2* was mainly enriched in cells in active cell cycle or malignant tumor cells. Subsequently, GSEA and *in vitro* experiments on human liver cancer cell lines with NCAPD2 overexpression or knockdown were adopted to investigate the biological features and molecular signaling pathways of NCAPD2 in liver cancer.

As a result, it was shown that NCAPD2 was prominently upregulated in liver cancer tissues compared with in control tissues based on clinical samples and datasets from the TNMplot, TCGA and ICGC databases. The association between *NCAPD2* and clinicopathological parameters in liver cancer revealed that *NCAPD2* expression was closely related to age, pTNM stage (especially T stage), histological grade and AFP levels. In addition, *NCAPD2* expression was closely related to poor OS and DSS, and could be considered an independent prognostic factor of OS in patients with liver cancer. Furthermore, *NCAPD2* expression was increased in *TP53* mut liver cancer compared with that in *TP53* wt liver cancer, but it was not related to the mutation status of *CTNNB1*. NCAPD2 expression was also positively correlated with the percentage of $Ki67^+$ cells in liver cancer. These findings indicated that NCAPD2 may be involved in cell proliferation in patients with liver cancer. Additionally, the GSEA of TCGA-liver cancer data validated that *NCAPD2* high expression was mostly enriched in tumor proliferation signature and G_2/M checkpoint of the cell cycle. Subsequently, HepG2 cells were selected for siRNA experiments and Huh7 cells were selected for overexpression experiments to further determine the biological roles of NCAPD2 in liver cancer. Consequently, overexpression of NCAPD2 enhanced tumor cell proliferation, invasion and cell cycle progression at the G_2/M-phase transition, and inhibited cell apoptosis in liver cancer cell lines.

c-Myc, as a member of the Myc family as well as a transcription factor, is a proto-oncogene that serves as a key regulator of the tumor microenvironment (TME) (32,33). c-Myc is involved in the regulation of diverse biological processes, including cell proliferation, differentiation, invasion and migration, and the recruitment of tumor cells, thus contributing to the regulation of angiogenesis and EMT (34). Moreover, c-Myc can affect the abundance of immune cell infiltration, specifically of natural killer cells, T cells and B cells, and the expression of programmed death cell protein (PD)-ligand 1/PD-1, thereby inducing immune evasion and immunosuppression (35). In turn, the TME can regulate c-Myc expression by various cytokines, the hypoxic microenvironment and factors released by tumor-associated fibroblasts (36). The PI3K-Akt-mTOR signaling pathway and related genes have been extensively studied, and have been shown to be related to multiple upstream and downstream elements of oncogenesis (37,38). Inhibition of this pathway has been proven to result in tumor regression in humans (39). Furthermore, PI3K-Akt-mTOR has been reported to dysregulate transcription factors, including c-Myc, to promote tumor survival and progression (40-42). Consequently, the *in vitro* assay demonstrated that the NCAPD2 overexpression promoted cell cycle progression at the G_2/M-phase transition, and activated the PI3K-Akt-mTOR/c-Myc signaling pathway and EMT progression, according to the analysis of Huh7 cells transfected with pcDNA-NCAPD2 overexpression plasmid (Fig. 7D).

In the present study, NCAPD2 expression was frequently upregulated in liver cancer tissues compared with in control liver tissues, and it was positively correlated with the percentage of $Ki67^+$ cells. Finally, the potential underlying biological mechanisms were identified, and it was suggested that NCAPD2 upregulation may promote cell cycle progression at the G_2/M-phase transition, and activate the PI3K-Akt-mTOR/c-Myc signaling pathway and EMT progression in liver cancer cells, thus augmenting tumor survival and progression. It may thus be hypothesized that NCAPD2 could be considered a promising prognostic marker or treatment target for liver cancer.

The present study has some limitations. Firstly, the sample size of patients with liver cancer was relatively small, and it is necessary to expand the sample size to confirm the aforementioned results. In addition, the underlying biological mechanism of *NCAPD2* in patients with liver cancer was mainly based on bioinformatics strategies and *in vitro* analyses of human liver cancer cell lines. Accordingly, *in vivo* research or even clinical trials on *NCAPD2* in liver cancer are still required. The academic field of structural biology has witnessed an increase in the application of high-resolution devices, such as cryo-electron tomography, due to rapid technical advancements in recent years. Understanding the precise macromolecular structures and mechanisms of each of

the individual functional modules of a cell helps researchers understand how cells work and the details of how genes function as a whole (43). Finally, regarding the evidence that PI3K-Akt-mTOR signaling is involved in NCAPD2-mediated liver cancer development, further studies are required to determine its direct pathogenic mechanism. Thus, for in-depth speculation, further investigation of the structural biology of NCAPD2 and related molecules is important for studying them as potential biotargets or therapeutic biomarkers for liver cancer.

In conclusion, in the present study, the upregulation of NCAPD2 in patients with liver cancer was comprehensively analyzed and may be used to predict an unfavorable prognosis based on the integrated findings of multiple public databases and clinical samples. Furthermore, NCAPD2 expression was positively correlated with the percentage of $Ki67^+$ cells, indicating that NCAPD2 might be involved in cell proliferation in patients with liver cancer. Finally, the *in vitro* assays demonstrated that overexpression of NCAPD2 led to cell cycle progression at the G_2/M-phase transition, and activation of the PI3K-Akt-mTOR/c-Myc signaling pathway and EMT progression in human liver cancer cells. Briefly, the current study has provided promising evidence for the function of NCAPD2 and its related signaling pathways in the initiation and progression of liver cancer, which may be used for developing potential biotargets or individualized therapeutic options for patients with liver cancer and high NCAPD2 expression.

Acknowledgements

Not applicable.

Funding

The present study was supported by the Hubei Provincial Natural Science Foundation (grant no. 2020CFB235).

Availability of data and materials

The publicly available data used in the present study may be found in TCGA (https://portal.gdc.cancer.gov/), TNMplot (https://tnmplot.com/), ICGC (https://icgc.org), the HPA (www.proteinatlas.org/) and IMMUcan (https://immucanscdb.vital-it.ch). The other data generated in the present study may be requested from the corresponding author.

Authors' contributions

JXG and YGH designed the study. YGH, PH and KH wrote the manuscript. JXG performed the *in vitro* assay. PH supervised the study and contributed to conception. YGH, KH and WLZ conducted the IHC assay and statistical analysis. XMZ contributed to the acquisition and interpretation of data. YQW participated in data collection, and provided helpful suggestions on method and figure preparation. SRY conducted data analysis and interpretation, revised the initial draft and provided suggestions for experimental design. All authors confirm the authenticity of all the raw data. All authors have read and approved the final version of the manuscript.

Ethics approval and consent to participate

The present study follows The Declaration of Helsinki. The current study was supported and approved by the Ethics Committee of Taihe Hospital (ethical approval no. 2024KS10; Shiyan, China). The samples involved in this study were obtained with written informed consent from patients or their families.

Patient consent for publication

Not applicable.

Competing interests

The authors declare that they have no competing interests.

References

1. Forner A, Reig M and Bruix J: Hepatocellular carcinoma. Lancet 391: 1301-1314, 2018.
2. Ganesan P and Kulik LM: Hepatocellular carcinoma: New developments. Clin Liver Dis 27: 85-102, 2023.
3. Llovet JM, Kelley RK, Villanueva A, Singal AG, Pikarsky E, Roayaie S, Lencioni R, Koike K, Zucman-Rossi J and Finn RS: Hepatocellular carcinoma. Nat Rev Dis Primers 7: 6, 2021.
4. Vogel A, Meyer T, Sapisochin G, Salem R and Saborowski A: Hepatocellular carcinoma. Lancet 400: 1345-1362, 2022.
5. Nagtegaal ID, Odze RD, Klimstra D, Paradis V, Rugge M, Schirmacher P, Washington KM, Carneiro F and Cree IA; WHO Classification of Tumours Editorial Board: The 2019 WHO classification of tumours of the digestive system. Histopathology 76: 182-188, 2020.
6. Zheng H, Pomyen Y, Hernandez MO, Li C, Livak F, Tang W, Dang H, Greten TF, Davis JL, Zhao Y, *et al*: Single-cell analysis reveals cancer stem cell heterogeneity in hepatocellular carcinoma. Hepatology 68: 127-140, 2018.
7. Friemel J, Rechsteiner M, Frick L, Böhm F, Struckmann K, Egger M, Moch H, Heikenwalder M and Weber A: Intratumor heterogeneity in hepatocellular carcinoma. Clin Cancer Res 21: 1951-1961, 2015.
8. Ball AR Jr, Schmiesing JA, Zhou C, Gregson HC, Okada Y, Doi T and Yokomori K: Identification of a chromosome-targeting domain in the human condensin subunit CNAP1/hCAP-D2/Eg7. Mol Cell Biol 22: 5769-5781, 2002.
9. Savvidou E, Cobbe N, Steffensen S, Cotterill S and Heck MM: Drosophila CAP-D2 is required for condensin complex stability and resolution of sister chromatids. J Cell Sci 118: 2529-2543, 2005.
10. Watrin E and Legagneux V: Contribution of hCAP-D2, a non-SMC subunit of condensin I, to chromosome and chromosomal protein dynamics during mitosis. Mol Cell Biol 25: 740-750, 2005.
11. Jing Z, He X, Jia Z, Sa Y, Yang B and Liu P: NCAPD2 inhibits autophagy by regulating Ca(2+)/CAMKK2/AMPK/mTORC1 pathway and PARP-1/SIRT1 axis to promote colorectal cancer. Cancer Lett 520: 26-37, 2021.
12. He J, Gao R, Yang J, Li F, Fu Y, Cui J, Liu X, Huang K, Guo Q, Zhou Z and Wei W: NCAPD2 promotes breast cancer progression through E2F1 transcriptional regulation of CDK1. Cancer Sci 114: 896-907, 2023.
13. Zhang Y, Liu F, Zhang C, Ren M, Kuang M, Xiao T, Di X, Feng L, Fu L and Cheng S: Non-SMC condensin I complex subunit D2 is a prognostic factor in triple-negative breast cancer for the ability to promote cell cycle and enhance invasion. Am J Pathol 190: 37-47, 2020.
14. Dong X, Liu T, Li Z and Zhai Y: Non-SMC condensin I complex subunit D2 (NCAPD2) reveals its prognostic and immunologic features in human cancers. Aging (Albany NY) 15: 7237-7257, 2023.
15. Bartha Á and Győrffy B: TNMplot.com: A web tool for the comparison of gene expression in normal, tumor and metastatic tissues. Int J Mol Sci 22: 2622, 2021.

16. Livak KJ and Schmittgen TD: Analysis of relative gene expression data using real-time quantitative PCR and the 2(-Delta Delta C(T)) method. Methods 25: 402-408, 2001.
17. Zeng D, Li M, Zhou R, Zhang J, Sun H, Shi M, Bin J, Liao Y, Rao J and Liao W: Tumor microenvironment characterization in gastric cancer identifies prognostic and immunotherapeutically relevant gene signatures. Cancer Immunol Res 7: 737-750, 2019.
18. Yoshihara K, Shahmoradgoli M, Martínez E, Vegesna R, Kim H, Torres-Garcia W, Treviño V, Shen H, Laird PW, Levine DA, *et al*: Inferring tumour purity and stromal and immune cell admixture from expression data. Nat Commun 4: 2612, 2013.
19. Bindea G, Mlecnik B, Tosolini M, Kirilovsky A, Waldner M, Obenauf AC, Angell H, Fredriksen T, Lafontaine L, Berger A, *et al*: Spatiotemporal dynamics of intratumoral immune cells reveal the immune landscape in human cancer. Immunity 39: 782-795, 2013.
20. Xiao Z, Dai Z and Locasale JW: Metabolic landscape of the tumor microenvironment at single cell resolution. Nat Commun 10: 3763, 2019.
21. Wei J, Huang K, Chen Z, Hu M, Bai Y, Lin S and Du H: Characterization of glycolysis-associated molecules in the tumor microenvironment revealed by pan-cancer tissues and lung cancer single cell data. Cancers (Basel) 12: 1788, 2020.
22. Camps J, Noël F, Liechti R, Massenet-Regad L, Rigade S, Götz L, Hoffmann C, Amblard E, Saichi M, Ibrahim MM, *et al*: Meta-analysis of human cancer single-cell RNA-seq datasets using the IMMUcan database. Cancer Res 83: 363-373, 2023.
23. Zhang Q, He Y, Luo N, Patel SJ, Han Y, Gao R, Modak M, Carotta S, Haslinger C, Kind D, *et al*: Landscape and dynamics of single immune cells in hepatocellular carcinoma. Cell 179: 829-845.e20, 2019.
24. Losic B, Craig AJ, Villacorta-Martin C, Martins-Filho SN, Akers N, Chen X, Ahsen ME, von Felden J, Labgaa I, D-Avola D, *et al*: Intratumoral heterogeneity and clonal evolution in liver cancer. Nat Commun 11: 291, 2020.
25. Verloh N, Probst U, Utpatel K, Zeman F, Brennfleck F, Werner JM, Fellner C, Stroszczynski C, Evert M, Wiggermann P and Haimerl M: Influence of hepatic fibrosis and inflammation: Correlation between histopathological changes and Gd-EOB-DTPA-enhanced MR imaging. PLoS One 14: e0215752, 2019.
26. Seipold S, Priller FC, Goldsmith P, Harris WA, Baier H and Abdelilah-Seyfried S: Non-SMC condensin I complex proteins control chromosome segregation and survival of proliferating cells in the zebrafish neural retina. BMC Dev Biol 9: 40, 2009.
27. Zhang P, Liu L, Huang J, Shao L, Wang H, Xiong N and Wang T: Non-SMC condensin I complex, subunit D2 gene polymorphisms are associated with Parkinson's disease: A Han Chinese study. Genome 57: 253-257, 2014.
28. Lin Y, Zeng C, Lu Z, Lin R and Liu L: A novel homozygous splice-site variant of NCAPD2 gene identified in two siblings with primary microcephaly: The second case report. Clin Genet 96: 98-101, 2019.
29. Yuan CW, Sun XL, Qiao LC, Xu HX, Zhu P, Chen HJ and Yang BL: Non-SMC condensin I complex subunit D2 and non-SMC condensin II complex subunit D3 induces inflammation via the IKK/NF-κB pathway in ulcerative colitis. World J Gastroenterol 25: 6813-6822, 2019.
30. Li Z, Zheng Y, Wu Z, Zhuo T, Zhu Y, Dai L, Wang Y and Chen M: NCAPD2 is a novel marker for the poor prognosis of lung adenocarcinoma and is associated with immune infiltration and tumor mutational burden. Medicine (Baltimore) 102: e32686, 2023.
31. Zhao Q, Zhang Y, Shao S, Sun Y and Lin Z: Identification of hub genes and biological pathways in hepatocellular carcinoma by integrated bioinformatics analysis. PeerJ 9: e10594, 2021.
32. Thompson EB: The many roles of c-Myc in apoptosis. Annu Rev Physiol 60: 575-600, 1998.
33. Meškytė EM, Keskas S and Ciribilli Y: MYC as a multifaceted regulator of tumor microenvironment leading to metastasis. Int J Mol Sci 21: 7710, 2020.
34. Dang CV: MYC on the path to cancer. Cell 149: 22-35, 2012.
35. Dhanasekaran R, Deutzmann A, Mahauad-Fernandez WD, Hansen AS, Gouw AM and Felsher DW: The MYC oncogene-the grand orchestrator of cancer growth and immune evasion. Nat Rev Clin Oncol 19: 23-36, 2022.
36. Gao FY, Li XT, Xu K, Wang RT and Guan XX: c-MYC mediates the crosstalk between breast cancer cells and tumor microenvironment. Cell Commun Signal 21: 28, 2023.
37. Janku F, Yap TA and Meric-Bernstam F: Targeting the PI3K pathway in cancer: Are we making headway? Nat Rev Clin Oncol 15: 273-291, 2018.
38. Alzahrani AS: PI3K/Akt/mTOR inhibitors in cancer: At the bench and bedside. Semin Cancer Biol 59: 125-132, 2019.
39. Peng Y, Wang Y, Zhou C, Mei W and Zeng C: PI3K/Akt/mTOR pathway and its role in cancer therapeutics: Are we making headway? Front Oncol 12: 819128, 2022.
40. Guo C, He J, Song X, Tan L, Wang M, Jiang P, Li Y, Cao Z and Peng C: Pharmacological properties and derivatives of shikonin-A review in recent years. Pharmacol Res 149: 104463, 2019.
41. Rebello RJ, Pearson RB, Hannan RD and Furic L: Therapeutic approaches targeting MYC-driven prostate cancer. Genes (Basel) 8: 71, 2017.
42. Nussinov R, Tsai CJ, Jang H, Korcsmáros T and Csermely P: Oncogenic KRAS signaling and YAP1/β-catenin: Similar cell cycle control in tumor initiation. Semin Cell Dev Biol 58: 79-85, 2016.
43. Beck M, Covino R, Hänelt I and Müller-McNicoll M: Understanding the cell: Future views of structural biology. Cell 187: 545-562, 2024.